BCG - Boletim de Ciências Geodésicas - On-Line version, ISSN 1982-2170
http://dx.doi.org/10.1590/S1982-21702015000300035

Artigo

USING SURFACE FITTING AND BUFFER ANALYSIS TO ESTIMATE REGIONAL GEOIDAL UNDULATION

Uso de ajustamento de superfície e análise de buffer para estimar a ondulação geoidal regional.

Fang-Shii Ning

Department of Land Economics, National Chengchi University.NO.64, Sec.2, ZhiNan Rd., Wenshan District, Taipei, Taiwan.Email:fsn@nccu.edu.tw

Abstract:

Geoidal undulation is the distance from the surface of an ellipsoid to the surface of a geoid measured along a line that is perpendicular to the ellipsoid. This paper describes how the geoidal undulation can be derived from the orthometric height, Global Navigation Satellite System geodetic height, and a surface model. Various surfaces fitting using the plane coordinates of the reference points and analysis with different buffers were used to determine the geoid undulation Taiwan. The results show that the quadratic surface model outperformed other surface models, yielding a buffer radius ranging from 15 to 25 km. According to the results, the accuracy of regional geoid undulation (city or state) can be improved through this process of surface fitting.

Keywords: Geoidal Undulation, Orthometric Height, Fitting Surface

Resumo:

A Ondulação geoidal é a distância entre as superfícies do elipsoide e do geoide, medido ao longo de uma linha que é perpendicular ao elipsoide. Este artigo descreve como a ondulação geoidal pode ser derivada a partir da altitude ortométrica, da altitude geodésica derivada do Sistema Global de Navegação por Satélite, e um modelo de superfície. Vários ajustamentos de superfície e análise com diferentes raios de buffer foram utilizados para determinar a ondulação geoidal de Taiwan. Os resultados mostram que o modelo de superfície quadrática apresentou melhor resultado com um raio do buffer variando de 15 a 25 km. De acordo com os resultados, a precisão da ondulação geoidal regional (cidade ou estado) pode ser melhorada por esse processo de ajustamento de superfície.

Palavra-chave: Ondulação Geoidal, Altitude Ortométrica, Ajustamento de Superfície

1. Introduction

Taiwan is an island in East Asia with a total area of approximately 3.6 million hectares.

Approximately 70% of Taiwan is covered with mountainous terrain. In the middle of Taiwan, the altitude of the highest point (Mt. Jade) is 3952 m. In Eastern Taiwan, the average height of the mountains near the coast is approximately 2000 m (Chen et al., 2011). The western area of Taiwan is predominantly a flat region (Figure 1). Obtaining the orthometric heights of benchmarks and monuments by using spirit levelling costs time and manpower. The geoidal undulation model can be used to solve this problem. The geoidal undulation can be computed using several techniques, for example, by using the numerical integration of Stokes' formula directly, fast Fourier transform, least squares collocation, spherical harmonic functions developed in a series, or by direct calculation of the difference between the ellipsoidal heights (from Global Navigation Satellite System – GNSS) and orthometric height (from spirit leveling)(Hwang et al., 2013).

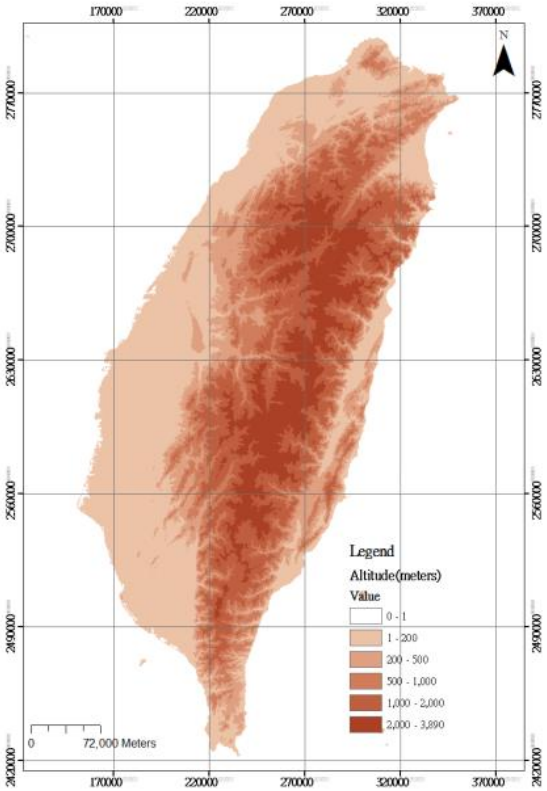

Figure 1 : Topographic map of Taiwan.

The ellipsoidal height provided by the GNSS is merely mathematics. In most studies, the height was referred to as the geoid. With sufficient level references with known horizontal and vertical coordinates, the geoid is almost always adjusted using the polynomials of least squares method, which enables the interpolation of geoidal undulations (Veronez et al., 2006). Numerous studies have combined various methods to improve the accuracy of models that employ the GNSS and geodetic levelling data to estimate local geoids (Abdalla and Tenzer, 2011; Lin, 2007; You, 2006; Featherstone et al., 2001).

In Taiwan, the data used for determining gravimetric geoid undulation included land gravity data and altimeter-derived sea surface gradient and shipborne gravity data. The gravimetric geoid

undulation was determined using the least squares method and the remove–restore technique by using a digital terrain model and digital density model of Taiwan. The precision of gravimetric geoid undulation is 18.8 cm in the flat area and 21.8cm in the mountainous area (Hwang and Wang, 2002). This precision is not adequate for high-accuracy surveying engineering; hence, geometric geoidal undulation was considered in this study.

This paper describes how the geoidal undulation of a point can be derived from the orthometric height, the GNSS geodetic height, and a surface model. Various surface models were tested to identify the optimal fitting surface and the appropriate surface-fitting buffer range for predicting Taiwan's geoidal undulation.

2. Methodology

The relationship between orthometric height (H) and geodetic height (h) is given by Equation 1 (Fotopoulos, 2003):

$$h \approx H + N \qquad (1)$$

where N represents the geoidal undulation.

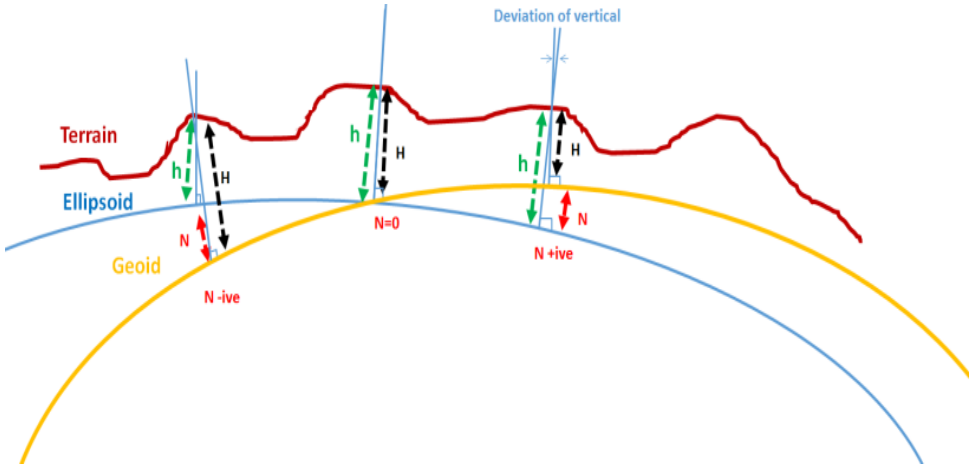

Figure 2 : Ellipsoidal and geoidal height (Smith, 1997).

2.1 Surface fitting

The polynomial method is one of the most widely used methods for expressing the study area as a single function. This method involves generating constant coefficients by using reference points with known values to form a geoid surface model; moreover, new points with unknown values can be calculated using these constant coefficients. High-order polynomial equations can be used to form a local geoid model by using the plane coordinates of the reference points as variables (Mevlut et al., 2011). In this study, various surface equations were used in analysis. The proposed surface

model can be used to classify planar, quadratic, cubic, quartic, and quintic surfaces, which are expressed in Equations 2–6, respectively (Awange et al., 2010). Such a surface model is required to account for datum inconsistencies and systematic distortions inherent amongst the various types of height data (Yang and Chen, 1999; Lancaster and Salkauskas, 1986). The plane surface equation is expressed in Equation 2.

$$N = a_0 + a_1 x + a_2 y + a_3 xy \quad (2)$$

$$N = a_0 + a_1 x + a_2 y + a_3 x^2 + a_4 y^2 + a_5 xy \quad (3)$$

$$N = a_0 + a_1 x + a_2 y + a_3 xy + a_4 x^2 + a_5 y^2 + a_6 x^3 + a_7 y^3 + a_8 x^2 y + a_9 xy^2 \quad (4)$$

$$N = a_0 + a_1 x + a_2 y + a_3 xy + a_4 x^2 + a_5 y^2 + a_6 x^3 + a_7 y^3 + a_8 x^2 y + a_9 xy^2 + a_{10} x^4 + a_{11} y^4 + a_{12} x^3 y + a_{13} x^2 y^2 + a_{14} xy^3 \quad (5)$$

$$N = a_0 + a_1 x + a_2 y + a_3 xy + a_4 x^2 + a_5 y^2 + a_6 x^3 + a_7 y^3 + a_8 x^2 y + a_9 xy^2 + a_{10} x^4 + a_{11} y^4 + a_{12} x^3 y + a_{13} x^2 y^2 + a_{14} xy^3 + a_{15} x^5 + a_{16} y^5 + a_{17} x^4 y + a_{18} x^3 y^2 + a_{19} x^2 y^3 + a_{20} xy^4 \quad (6)$$

where a_n denotes unknown parameters, N indicates the geoidal undulation, and x and y indicate the components on the abscissa and ordinate, respectively.

The comparison chart in Figure 3 depicts the training sample errors and test sample errors obtained using models of varying complexities employing 100 sets of training data with 50 samples in each set (Hastie et al., 2009). In the figure, the abscissa and ordinate indicate the model complexity and prediction error; the pale blue and reddish curves indicate the training errors and test errors; and the solid and dashed lines indicate the predicted training and test errors, respectively. The graph shows that models of higher complexity yielded fewer training errors and test errors. However, as the model became more complex, the distance from the test errors increased. Because the complexity increased until the training error reached zero, overfitting of the training samples occurred.

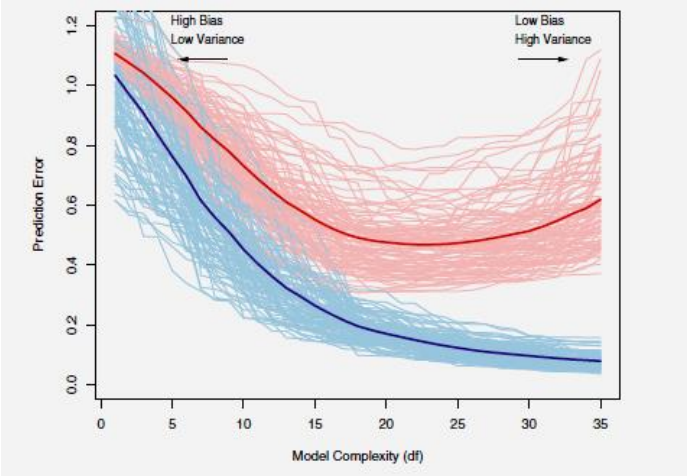

Figure 3 : Training sample errors and test sample errors under different model complexities (Hastie et al., 2009)

The aforementioned simulation data show that the model complexity indicates the order of the surface equation, whereas the training error indicates the degree of internal precision. Using a higher-order surface equation reduces the internal precision but increases the test errors (i.e., the prediction errors of the model). Thus, a mechanism for evaluating the prediction errors is necessary.

2.2 Buffer Analysis

Circular buffer zones are widely used in various types of environmental analysis (Chakraborty and Armstrong, 1997). This study investigated methods for determining the proper range for fitting a geoidal undulation. Determining the proper range involves analyzing the buffer on the basis of the optimal fitting surface. As shown in Figure 4, a known point is first selected as the center of a circle with a given radius (i.e., the proper range). A search is then performed for all known points in the circle. Finally, these points are used to determine the optimal surface according to an evaluation of the results.

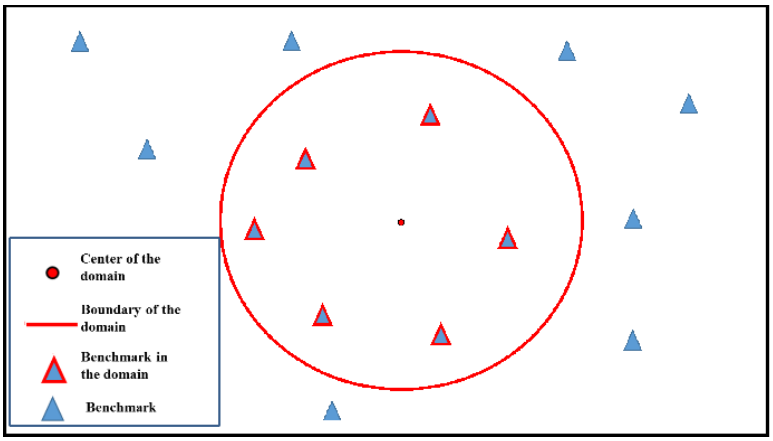

Figure 4 : Schematic of a buffer analysis.

A buffer analysis was conducted using the following different radii: 5, 10, 15, 20, 25, and 30 km.

According the principle of the first-order benchmark levelling measurement standards, the benchmarks should be spaced an average of 2 km from each other (Ministry of the interior, 2014).

Based on this principle, if the measured points are close to other levelling lines, then the fitting range of a 5-km radius would have six points, which are sufficient for solving a quadratic surface equation. The first-order benchmarks of Taiwan are along a highway and can be covered using a buffer analysis of 5, 10, and 15-km annulus distances, as shown in Figure 5.

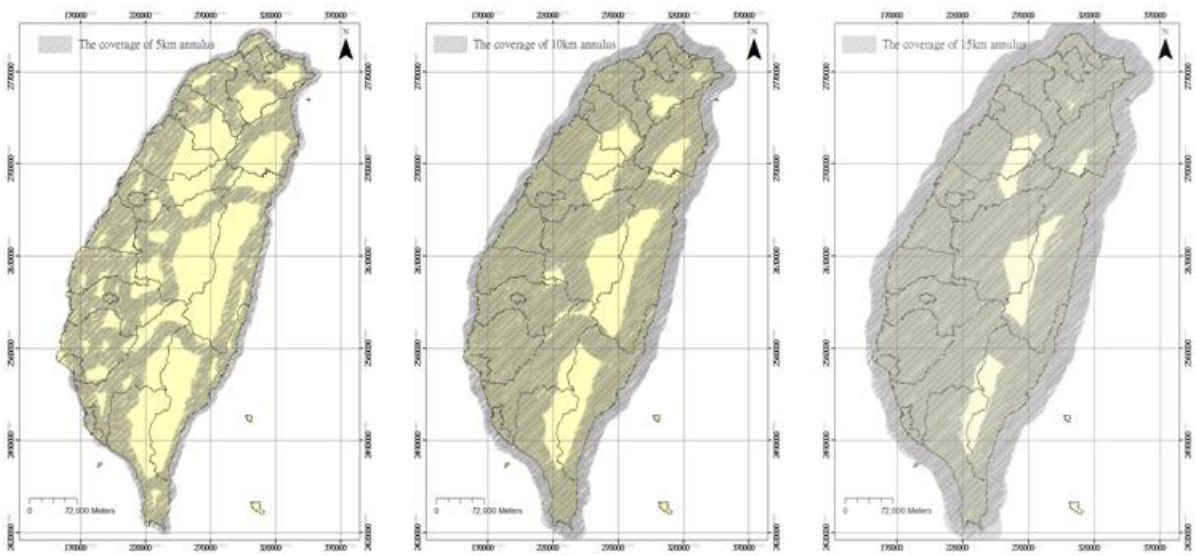

Figure 5 : Coverage of using a 5, 10, and 15-km radii buffer analysis.

3. Data and Results

3.1.1 Data on Surface Fitting

In this study, 78 GPS observations on the benchmarks of the spirit levelling network in Taichung City were combined with the point distribution profile shown in Figure 6. These data were used because the distribution of these points is relatively uniform throughout Taichung City, and they are ideal data for fitting the geoidal undulation.

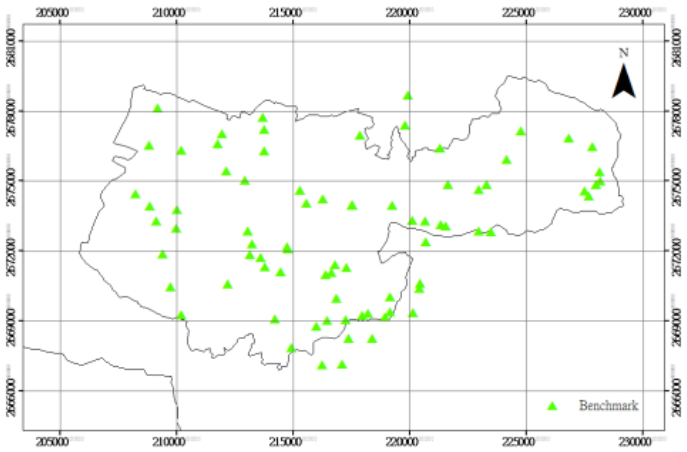

Figure 6 : Distribution of levelling data.

Planar, quadric, cubic, quartic, and quintic surface models (Equations 2–6, respectively) were used

to fit the geoidal undulation values in the Taichung experimental area. The experiment was conducted to obtain the optimal surface model for fitting the data. Figure 7 is a flow chart of the suface fitting process employed in this study.

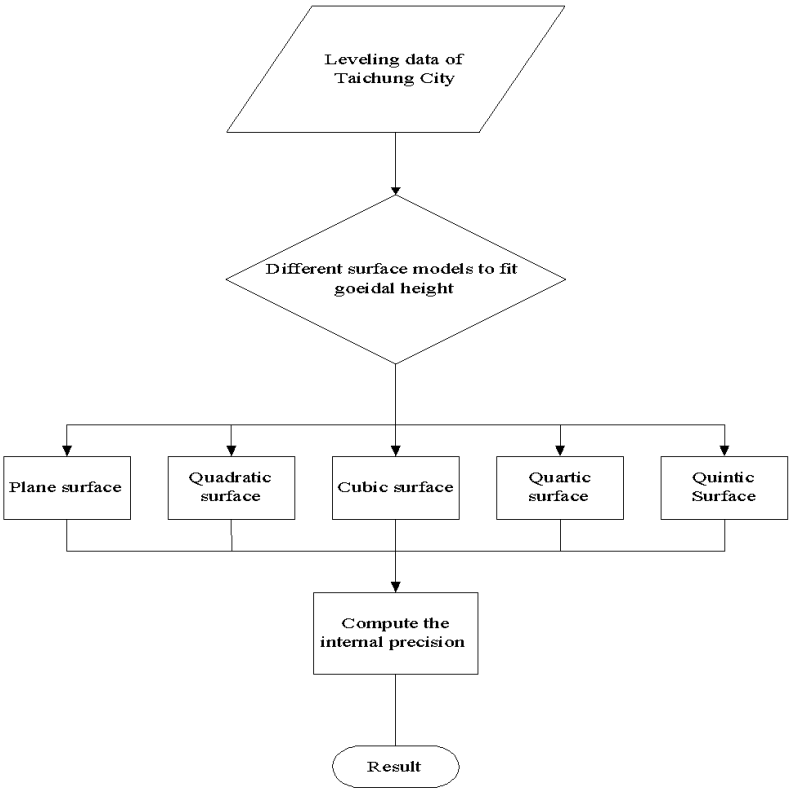

Figure 7 : Flow chart of the surface model analysis.

3.1.2 Data for Buffer Analysis

This study used 2067 first-order Class I and II benchmarks that were surveyed and calculated by the National Land Surveying and Mapping Center (Figure 8). The first-order levelling line misclosure limit in Taiwan for the Class I benchmarks is 2.5 mm, and that of the Class II benchmarks is 3.0 mm, where K is the distance of the levelling line (in kilometers). All levelling height differences were corrected by performing collimation error, refraction error, curvature, orthometric, temperature, and rod-scale corrections. Table 1 shows a summary of the estimated standard deviation of the unit weight of the levelling height network adjustment; the precision of the levelling heights, and the precision of the levelling height differences. The average precision of the levelling height differences was in agreement with the second-order Class I elevation accuracy standard of the Federal Geodetic Control Committee vertical control network (FGCC, 1984). The benchmark coordinates were obtained using GPS positioning techniques, which, for the Class I benchmarks, were performed using dual-frequency GPS receivers for at least 2 hours, and for at least 3 hours for the Class II benchmarks (Yang et al., 2001). Table 1 shows the precision of the GPS-derived ellipsoidal heights and that of the GPS-derived ellipsoidal height differences. The precision of the height differences is in agreement with the relative positioning accuracy standard of Order B (FGCC, 1988).

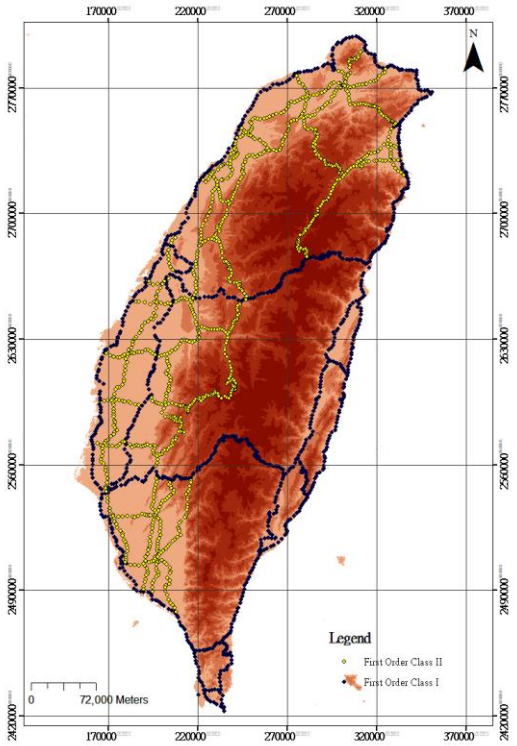

Figure 8 : The distribution of 2067 first-order Class I and II benchmarks.

Table 1 : Statistics of the first-order height network

	First-order network	
Parameter	Class I	Class II
Number of benchmarks used	1013	1054
$\hat{\sigma}_0$	$\pm 0.73\sqrt{K}$ mm	$\pm 0.75\sqrt{K}$ mm
Precision of leveling heights		
Maximum	±11.1 mm	±2.3 mm
Mean	±9.0 mm	±8.8 mm
Precision of leveling height differences		
Maximum	±1.6 mm	±13.1 mm
Mean	±1.0 mm(or ±0.5 ppm)	±1.0 mm(or ±0.6 ppm)
Precision of GPS ellipsoidal heights		
Maximum	±15.6 cm	±4.1 cm
Mean	±4.7 cm	±1.4 cm
Precision of GPS ellipsoidal height differences		
Maximum	±18.8 cm	±5.6 cm
Mean	±5.5 cm(or ±0.8 ppm)	±1.7 cm(or ±0.3 ppm)

3.2.1 Results of Surface Fitting

Figure 9 shows the experimental results; the precisions of the planar, quadratic, cubic, quartic, and quintic surface models were 5.57, 2.25, 2.04, 2.01, and 1.97 cm, respectively. The experimental results are nearly consistent with those shown in Figure 2. As the model increased in complexity, the precision decreased gradually, approaching 0; however, the prediction errors fluctuated when valleys were reached and the model complexity decreased. Although the most complex model in the experiment was only a quintic surface equation, it is reasonable to estimate that the precision of a higher-order surface equation would be less than 1.97 cm. The figure shows that the model precisions were the closest between the quadratic and quartic surface models.

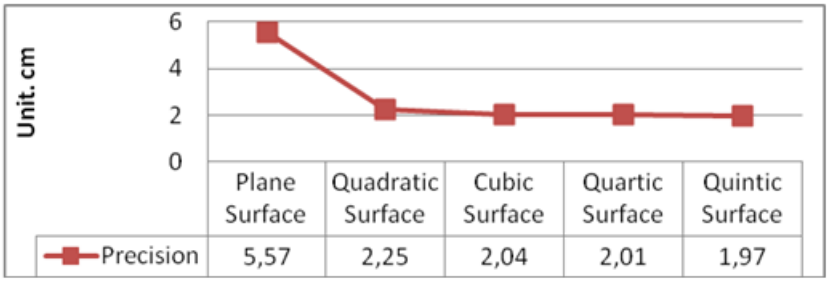

Figure 9 : Precisions of different surface fitting (Taichung experimental area).

However, the quartic equation requires 15 observations, which is considerably more than the 6 and 10 required for the quadratic and cubic surface equations, respectively. Considering the potentially lower density of the benchmarks distributed over Taiwan compared with those in the Taichung experimental area, 15 or more observations must be present in the fitting range, which is difficult.

The obtained fitting results indicated that the increase was not large. Consequently, there is no reason to accept the quartic surface equation. Therefore, for the sake of parsimony, the quadratic surface method is optimal for determining regional geoidal undulation.

3.2.2 Results of Buffer Analysis

The proper range for fitting geoidal undulation is based on the optimal fitting surface, which is the quadratic surface model. In this study, the trial area was Taiwan, and 2067 benchmarks were used.

We used 5-, 10-, 15-, 20-, 25-, and 30-km buffer radii to determine the number of known benchmarks in the buffer area, and the results are shown in Table 2. The average number of points in the 5-km-radius buffer area was 9.2 (minimum = 3); thus, only a few areas could not be processed. A buffer radius ranging from 10 to 30 km can cover most of Taiwan.

Table 2 : Numbers of benchmarks in different buffer radii

Buffer radius	Average points	Maximum points	Minimum points
5 km	9.2	21	3
10 km	24.2	47	9
15 km	44.8	82	15
20 km	70.3	118	21
25 km	100.1	168	28
30 km	134.0	226	40

The precisions of the levelling and ellipsoidal heights were 9 and 4.7 cm, respectively (Table 1), and applying error propagation yielded a precision of 5 cm. Consequently, the results were classified in every 5 cm. Table 3 shows the generated precision computed from the fitting process based 2067 benchmarks. Table 4 lists the precisions of the fitting surfaces that were higher than 5 cm in various radii.

Table 3 : The fitting precision in different buffer radii using 2067 benchmarks.

Precision	5km	10km	15km	20km	25km	30km
<5 cm	527	1513	1672	1446	1231	443
5 cm-10 cm	90	174	306	583	736	1343
10 cm -15 cm	44	81	48	34	100	256
15 cm - 20 cm	44	23	5	3	0	25
>20 cm	1362	276	36	1	0	0

Table 4 : Precisions of better than 5-cm fitting precision in different buffer radii

Buffer radius	5km	10km	15km	20km	25km	30km
Mean precision (cm)	1.9	2.4	3.0	3.5	3.8	4.1

Tables 3 and 4 show that the number of points yielding precision values less than 5 cm ranged from 443 to 1672 in various radii. Particularly, 80% of the 2067 points in the 15-km radius yielded precision values less than 5 cm. However, the 5- and 30-km-radius fitting results were unfavorable, yielding only 527 and 443 points with precision values less than 5 cm, respectively. The number of points with precision values smaller than 5 cm in the 10-, 15-, 20-, and 25-km buffer radii accounted for 73%, 81%, 70%, and 60% of all points and yielded mean precision values of 2.4, 3.0, 3.5, and 3.8 cm, respectively. The surface-fitting precision values less than 10 cm accounted for 82%, 96%, 98%, and 95% of all points; however, the precision at some points was less than 20 cm (specifically, 1362 points in the 5-km buffer radius and 276 points in the 10-km buffer radius). This occurred because there were fewer benchmarks and the figure strength was weakly distributed. The areas with an insufficient number of benchmarks (Figure 10) yielded unfavorable fitting surface results.

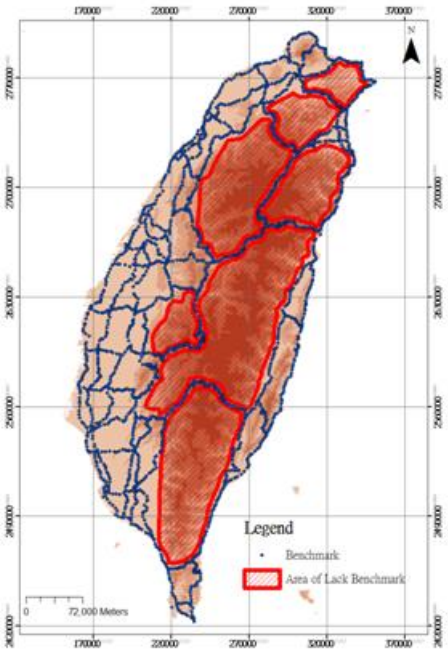

Figure 10 : Areas that lack benchmarks.

The fitting surface precision values along the northeast coastline were rough because the benchmarks had a linear rather than surface distribution and few points were located in the mountain area (Figure 11). Consequently, in this area, it was difficult to locate a suitable 5-km buffer radius with a sufficient number of benchmarks for the fitting surface.

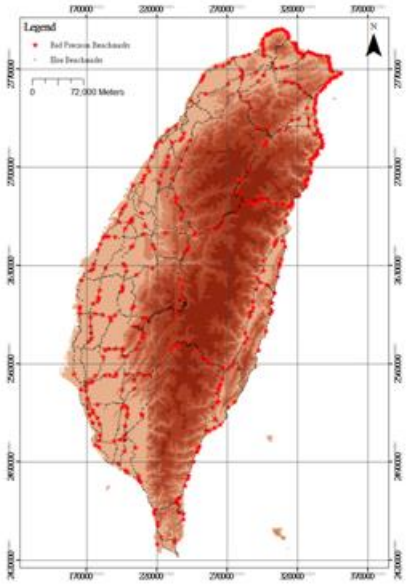

Figure 11:Unfavorable precision benchmarks.

4. Conclusion

Taiwan is characterized by complex terrain; therefore, the experimental results can be applied to all terrains and countries. The experimental results show that the quadratic surface method is optimal for determining regional geoidal undulation. The results also show that a buffer radius between 10 and 25 km can yield precision values smaller than 5 cm at 60% to 80% of points and precision values of 10 cm at 82% to 98% of points. Therefore, the proposed method is effective for predicting geometric geoid undulation with adequate precision. According to these findings, high-accuracy regional (city or state) geoidal undulation can be predicted.

ACKNOWLEDGMENTS

The author thanks the anonymous reviewers for their constructive comments which significantly improved the quality of the original article.

REFERENCES

Abdalla, Ahmed; and Tenzer, Robert. "The evaluation of the New Zealand's geoid model using the KTH method." *Geodesy and Cartography* 37.1 (2011): 5-14.

Awange, J. L., Grafarend, E. W., Paláncz, B., & Zaletnyik, P. Algebraic geodesy and geoinformatics. Springer Science & Business Media, 2010.

Chakraborty, Jayajit, and Armstrong, Marc P.. "Exploring the use of buffer analysis for the identification of impacted areas in environmental equity assessment." Cartography and Geographic Information Systems 24.3 (1997): 145-157.

Chen, Kwo-Hwa, M. Yang , Y. T. Huang, K. E. Ching, & Rau, R. J.. "Vertical displacement rate field of taiwan from geodetic levelling data 2000-2008." Survey Review 43.321 (2011): 296-302.

Featherstone, W., Kirby, J., Kearsley, A., Gilliland, J., Johnston, G., Steed, J. & Sideris, M. "The AUSGeoid98 geoid model of Australia: data treatment, computations and comparisons with GPS-levelling data." Journal of Geodesy 75.5-6 (2001): 313-330.

Fotopoulos, Georgia. 2003. An analysis on the optimal combination of geoid, orthometric and ellipsoidal height data. University of Calgary, Department of Geomatics Engineering.

Federal Geodetic Control Committee (FGCC). 1984. Standards and specifications for geodetic control networks. Rockville, Md.

Federal Geodetic Control Committee (FGCC). 1988. Geometric geodetic accuracy standards and specifications for using GPS relative positioning techniques, Rockville, Md.

Hwang, C, H.J. Hsu, and Huang, C.. "A New Geoid Model of Taiwan : Applications to Hazard

Mitigation, Environmental Monitoring and Height Modernization." Taiwan Journal of Geoinformatics 1.1(2013):57-81. (in Chinese).

Hwang, C., and Wang, C.G.. "New gravity anomaly grid of Taiwan." Journal of Surveying Engineering 44.2(2002):1-22. (in Chinese).

Hastie, Trevor.,et al. The elements of statistical learning. New York: Springer, 2009.

Lin, Lao-Sheng. "Application of Back-Propagation Artificial Neural Network to Regional Grid-Based Geoid Model Generation Using GPS and Leveling Data." *Journal of Surveying Engineering*133. 2(2007):81-89.

Lancaster, P. and Salkauskas, K. Curve and surface fitting. Academic press, 1986.

Mevlut, Gullu, Mustafa Yilmaz, and Yilm, Ibrahim. "Application of Back Propagation Artificial Neural Network for Modelling Local GPS/Levelling Geoid Undulations: A Comparative Study." In: TS07C - Geoid and GNSS Heighting, FIG Working Week 2011 Bridging the Gap between Cultures, Marrakech, Morocco, 18-22 May 2011.

Ministry of the interior. 2014. The Specification of The First-Order Levelling.(in Chinese).

Smith, James R. Introduction to geodesy: the history and concepts of modern geodesy. John Wiley & Sons, 1997.

Veronez, M. R. Thum, A.B. and Souza, G. C. "A new method for obtaining geoidal undulations through Artificial Neural Networks." Proceedings of 7 th International Symposium on Spatial Accuracy Assessment in Natural Resources and Environmental Sciences, Lisbon, Portugal. 2006.

Yang, Ming, Ching-Liang Tseng and Yu, Jyh-Yih. "Establishment and maintenance of Taiwan geodetic datum 1997. " *Journal of surveying engineering* 127.4(2001): 119-132.

You, Rey-Jer. " Local geoid improvement using GPS and leveling data: Case study." *Journal of surveying engineering* 132.3(2006):101-107.

Yang, Zhan-Ji and Chen, Yong-Qi. " Determination of local geoid with geometric method: Case study. " *Journal of surveying engineering* 125.3(1999): 136-146.

Recebido em março de 2015. Aceito em abril de 2015.